

Rotational spectra and hyperfine constants of ZrO and ZrS

Sara A. Beaton and Michael C. L. Gerry

Citation: *The Journal of Chemical Physics* **110**, 10715 (1999); doi: 10.1063/1.479014

View online: <http://dx.doi.org/10.1063/1.479014>

View Table of Contents: <http://scitation.aip.org/content/aip/journal/jcp/110/22?ver=pdfcov>

Published by the [AIP Publishing](#)

Articles you may be interested in

[Rotational spectra of rare isotopic species of fluoriodomethane: Determination of the equilibrium structure from rotational spectroscopy and quantum-chemical calculations](#)

J. Chem. Phys. **137**, 024310 (2012); 10.1063/1.4731284

[Internuclear distance and effects of Born–Oppenheimer breakdown for PtS, determined from its pure rotational spectrum](#)

J. Chem. Phys. **121**, 3486 (2004); 10.1063/1.1769365

[Rotational spectrum of jet-cooled HfO 2 and HfO](#)

J. Chem. Phys. **117**, 9651 (2002); 10.1063/1.1516797

[Fourier transform microwave rotational spectra of the Ne 2 –N 2 O and Ar 2 –N 2 O van der Waals trimers](#)

J. Chem. Phys. **111**, 3919 (1999); 10.1063/1.479695

[Fourier-transform microwave spectrum, structure, harmonic force field, and hyperfine constants of sulfur chloride fluoride, CISF](#)

J. Chem. Phys. **106**, 10037 (1997); 10.1063/1.474061



Rotational spectra and hyperfine constants of ZrO and ZrS

Sara A. Beaton and Michael C. L. Gerry^{a)}

Department of Chemistry, The University of British Columbia, 2036 Main Mall, Vancouver, British Columbia, Canada V6T 1Z1

(Received 9 November 1998; accepted 5 March 1999)

The pure rotational spectra of ZrO and ZrS have been recorded using cavity Fourier transform microwave spectroscopy in the frequency range 9–26 GHz. The molecules were generated by laser ablation of a solid Zr rod in the presence of 0.05% of O₂ or H₂S, respectively, in either argon or neon. Rotational spectra of five previously unobserved isotopomers of ZrO in the $X^1\Sigma^+$ state have been measured. Spectra for all five Zr³²S isotopomers and for the ⁹⁰Zr³⁴S isotopomer in natural abundance have also been measured; this is the first report of pure rotational transitions for ZrS. Transitions in several excited vibrational states were also measured for the most abundant isotopomers of both species. Atomic mass-dependent Born–Oppenheimer breakdown correction terms were determined by fitting the data obtained for each molecule to a Dunham-like expression. Values for the equilibrium bond lengths of the two species were also calculated from the results of these fits. For both the ⁹¹Zr³²S and ⁹¹Zr¹⁶O isotopomers, nuclear hyperfine structure due to the zirconium nucleus was observed and values for $eQq_0(^{91}\text{Zr})$ and $C_1(^{91}\text{Zr})$ have been determined. A rotational transition in the low lying $a^3\Delta$ state of ZrS has also been observed. © 1999 American Institute of Physics. [S0021-9606(99)00121-X]

I. INTRODUCTION

In general, the transition metal monosulphides have been less well characterized than the analogous monoxides. Chemically, both species are models for understanding transition metal bonding involving d electrons. Measuring the spectroscopic properties of these molecules, particularly hyperfine parameters, can therefore give valuable insight into their electronic structures and the nature of the chemical bonds involved. The majority of the work to date on these species has been electronic spectroscopy. However, these diatomic molecules often have surprisingly complicated electronic spectra, and the analysis may be far from straightforward.¹ Such molecules typically have a large number of low lying electronic states with high spin multiplicities and perturbed excited electronic states; in addition many transition metal nuclei have nuclear spins. To add to this, the molecules can be difficult to generate in the gas phase because of the refractory nature of many transition metals and their compounds. In terms of theoretical calculations, electron correlation effects become important when there are many unpaired electrons and so these molecules also provide a challenge for *ab initio* techniques. Spectroscopic data can therefore be used to calibrate these calculations for such systems. The combination of the above considerations with the fact that only a handful of these molecules have Σ ground states has resulted in only a few transition metal monoxides and no monosulphides having been studied by Fourier transform microwave (FTMW) spectroscopy.

In addition to fundamental spectroscopic interest in these species, both ZrO and ZrS are molecules of considerable

astrophysical importance. Many transition metal oxides and hydrides [e.g., TiO (Ref. 2), LaO (Ref. 3), and FeH (Ref. 4)] have been detected via their electronic spectra in cool, carbon rich stars (M and S type). However, recent calculations have predicted that in such environments where the C:O ratio is close to unity, certain metal monosulphides including ZrS may be more abundant than the corresponding metal monoxides.⁵ More detailed knowledge of the composition of the atmospheres of these stars is required to further the understanding of stellar evolution. The absorption bands of ZrO were first detected in S -type stars in 1922,⁶ and now constitute a defining characteristic of such stars. Consequently ZrO has received a vast amount of spectroscopic attention including optical (for example Refs. 7, 8) and microwave⁹ studies, *ab initio* calculations,^{10,11} lifetime studies,¹² and rotational line strength analyses.¹³ In contrast, it is only in the last decade that ZrS has been identified as the carrier of the Keenan bands [three red degraded bands first observed in 1950 (Ref. 14) in the spectra of certain S -type stars], thus confirming its presence in these stellar atmospheres. This was largely due to the fact that when ZrS was first proposed as the carrier of the Keenan bands in 1980 (Ref. 5) there were no laboratory spectroscopic data available for this molecule.

Zr has five naturally occurring isotopes: ⁹⁰Zr(51.45%), ⁹¹Zr(11.22%), ⁹²Zr(17.15%), ⁹⁴Zr(17.38%), and ⁹⁶Zr(2.80%). Only the ⁹¹Zr nucleus has nuclear spin, with $I = 5/2$. Accurate spectroscopic constants for the $X^1\Sigma^+$ state of ZrO are known from a variety of studies. B_e , α_e , and γ_e were determined for ⁹⁰Zr¹⁶O in an extensive analysis of the vibrationally excited bands of the $B^1\Pi - X^1\Sigma^+$ electronic transition by Philips and Davis.⁷ More recently, Simard *et al.*¹⁵ re-examined the $C^1\Sigma^+ - X^1\Sigma^+$ transition via laser induced fluorescence using a laser ablation/supersonic ex-

^{a)}Author to whom correspondence should be addressed; electronic mail: mgerry@chem.ubc.ca

pansion technique. Rotational constants for all five $Zr^{16}O$ isotopomers were obtained in this work. Also, the FTMW spectra of $^{90}Zr^{16}O$, $^{92}Zr^{16}O$, and $^{94}Zr^{16}O$ have been measured by Suenram *et al.*⁹ by ablating a rod of ZrO_2 and using pure Ne backing gas. The authors stated in Ref. 9 that the signals obtained were not strong enough to permit measurements of the two remaining minor isotopomers.

The first published spectroscopic study of ZrS was by Simard *et al.* in 1988.¹⁶ They observed the $E^1\Sigma^+ - X^1\Sigma^+$ transition in the visible region of the spectrum by laser induced fluorescence. The molecule was made by laser ablation of a zirconium rod with a few percent of OCS in a helium backing gas. A vibrational analysis of the main isotopomer was given; however the resolution of the spectrum did not permit a rotational analysis. Also in 1988, Jonsson, Lindgren, and Taklif¹⁷ reported in a letter that they had observed two singlet bands and several triplet bands (including the $b^3\Phi - a^3\Delta$ transition which gives rise to the Keenan bands) in emission at high resolution. In this case, they used a microwave discharge through $ZrCl_4$ and sulphur in argon to make ZrS. A preliminary bond length for the ground state was given in Ref. 17, and rotational analyses of three triplet bands for the main isotopomer were subsequently published in 1995.^{18,19} Since then, a full rotational analysis of the singlet bands has also been performed,²⁰ although we were unaware of the results of that work at the outset of this study. There is also a very recent lifetime study of the singlet states of zirconium sulphide.²¹ In addition, there has been an *ab initio* study performed by Langhoff and Bauschlicher on several transition metal oxides and sulphides which included both ZrS and ZrO.¹⁰

In this article we report the observation of the pure rotational spectra of the $X^1\Sigma^+$ states of ZrO and ZrS, measured using cavity pulsed FTMW spectroscopy. Previous work on ZrO has been extended and rotational transitions have been measured for a further five isotopomers. For ZrS, this is the first observation of the rotational spectrum; transitions have been observed for six isotopomers in natural abundance. The data obtained for ZrO and ZrS have been fit to a Dunham-like expression and Born–Oppenheimer breakdown correction terms have been determined in each case. Equilibrium bond lengths have been calculated for both molecules. For both the $^{91}Zr^{32}S$ and $^{91}Zr^{16}O$ species, nuclear hyperfine structure in the ground state has been observed for the first time, and the nuclear quadrupole coupling constants for ^{91}Zr have been determined. In addition, a rotational transition in the low lying $a^3\Delta$ state of ZrS has been observed and is discussed.

II. EXPERIMENT

A Balle–Flygare-type Fourier transform microwave spectrometer²² was used to measure the spectra of ZrO and ZrS. This instrument has been described in detail elsewhere²³ and only a brief description will be given here. The microwave cavity consists of two spherical aluminum mirrors 24 cm in diameter, with a radius of curvature of 38.4 cm, placed approximately 30 cm apart. One of the mirrors is movable so that the cavity can be tuned into resonance at the microwave

excitation frequency. A pulsed nozzle is mounted near the center of the other, fixed mirror. All measured lines appear as doublets due to the Doppler effect, since the molecular jet and the axis of microwave propagation are parallel. Operating the spectrometer in this “parallel configuration” provides high sensitivity and very narrow linewidths, the latter on the order of 9–10 kHz full width at half maximum (FWHM). The measurement accuracy is estimated to be better than ± 1 kHz.

The laser ablation source used to generate gas phase ZrO and ZrS samples has also been described previously.²⁴ A stainless steel nozzle cap was used to hold a 5 mm diam Zr rod (Goodfellow, 99.8+%) approximately 5 mm from the orifice of a General Valve Series 9 nozzle. The rod was continuously rotated and translated to expose a fresh area of the surface to each laser pulse. The second harmonic of a Q-switched Continuum Surelite I (Nd:YAG) laser was used to ablate the zirconium rod (~ 5 mJ per pulse @ 532 nm). The laser pulse was timed to coincide with a gas pulse of a suitable reactant molecule in a buffer gas which then underwent supersonic expansion into the microwave cavity. The nozzle typically operated with a backing pressure of 4–6 atm. The repetition rate of the experiment was 1 Hz.

Strong ZrO signals (which did not become weaker over time) could be readily observed using pure argon as a backing gas; such experimental conditions for making metal oxides have been observed before.²⁵ Adding small amounts of O_2 to the argon produced, at best, a 50% increase in signal strength. The signals were such that the $J=1-0$ transition of the main isotopomer could be observed in two averaging cycles. It is likely that ZrO arises from ZrO_2 present in the rod as an impurity, but also that a small amount forms from O_2 (not H_2O) as an impurity in the backing gas sample. The latter is supported by two qualitative observations: (a) using 0.05% O_2 (50% ^{18}O) in the argon backing gas produced “strong” $Zr^{18}O$ signals, (b) using 0.05% H_2O (40% ^{18}O) produced only “very weak” $Zr^{18}O$ signals. The $Zr^{16}O$ and $Zr^{18}O$ $v=0$ spectra reported here were measured using conditions similar to (a) above. ZrS was produced by reacting ablated metal plasma with 0.05% H_2S in argon backing gas. This was found to give about four to five times better signal to noise than using OCS in argon as a source of sulphur. The best ZrS signals obtained were approximately five times weaker than the corresponding ZrO signals. In order to observe rotational transitions in excited vibrational states for both species, neon was used as the backing gas instead of argon. This produced a higher vibrational temperature in the expansion without significantly reducing the rotational cooling; see later for details. Neon was also used in the measurement of transitions in the $a^3\Delta$ excited electronic state of ZrS.

III. RESULTS

A. ZrO ($X^1\Sigma^+$ state)

As was mentioned in the introduction, microwave spectra of the $J=1-0$ transition in the $X^1\Sigma^+$ state have been measured previously for the three most abundant ZrO

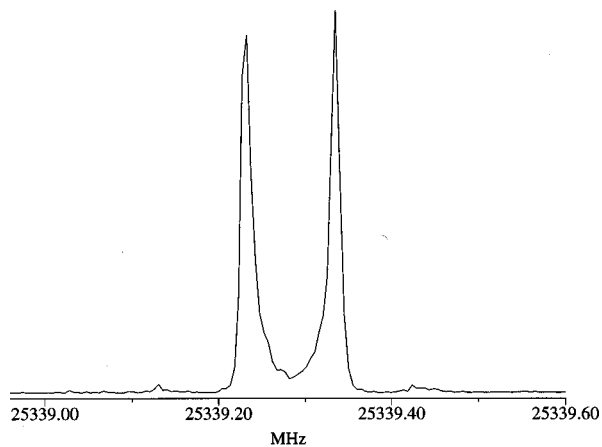


FIG. 1. Power spectrum of the $J=1-0$ $v=0$ transition of $^{90}\text{Zr}^{16}\text{O}$ measured in 100 averaging cycles. The excitation frequency was 25 339.2820 MHz. 4 K data points were recorded and the power spectrum is shown as a 4 K transformation. For this measurement the backing gas used was pure argon.

isotopomers.⁹ This was also the only rotational transition available in the frequency range of our spectrometer. The frequencies of these three transitions remeasured in the present work are reported for completeness. A typical spectrum is shown in Fig. 1. The transition frequencies for the other isotopomers were predicted by mass scaling the rotational constant and the literature value of D_0 for the main isotopomer (see Table IV). For $^{91}\text{Zr}^{16}\text{O}$, the only guide to the magnitude of the hyperfine splitting was that it had not been resolved in the laser induced fluorescence study,¹⁵ in which linewidths of 120 MHz were obtained. All three hyperfine components of the $J=1-0$ $v=0$ transition of $^{91}\text{Zr}^{16}\text{O}$ were observed, as well as $J=1-0$ $v=0$ transitions of $^{96}\text{Zr}^{16}\text{O}$ and three Zr^{18}O isotopomers. From the molecular constants in Ref. 7, the frequencies of the $J=1-0$ rotational transitions in excited vibrational states for a number of isotopomers were predicted. With neon as the backing gas, the signals were sufficiently strong and the vibrational temperature of the expansion sufficiently high ($T_{\text{vib}} \sim 650$ K) that transitions up to $v=3$ were measured for the main isotopomer and up to $v=2$ for several other isotopic species. Table I gives the complete list of the measured transition frequencies for ZrO.

B. ZrS ($X^1\Sigma^+$ state)

Only the $J=1-0$ and $J=2-1$ transitions in the $X^1\Sigma^+$ state of ZrS were available in the frequency range of the spectrometer. Using the preliminary bond length of 2.156 Å reported by Jonsson, Lindgren, and Taklif¹⁷ an initial prediction for the $J=1-0$ transition frequency for the main isotopomer was made. The transition was found within 20 MHz of this frequency. Its identity was confirmed by observing transitions for the four other Zr^{32}S isotopomers and the $^{90}\text{Zr}^{34}\text{S}$ isotopomer in natural abundance. The frequencies of $J=1-0$ transitions of the minor isotopomers were predicted by simply mass scaling B_0 for the main isotopomer, and all the unsplit transitions were found within 500 kHz of the predictions. For the $^{91}\text{Zr}^{32}\text{S}$ isotopomer, hyperfine structure due to the zirconium nucleus was observed. The spectral searches for the hyperfine components were based on the

TABLE I. Measured frequencies for the $J=1-0$ transition of ZrO in the $X^1\Sigma^+$ state.

Isotopomer	$F'-F''$	v	Frequency (MHz)	obs-calc (kHz) ^a	Ref. 9
$^{90}\text{Zr}^{16}\text{O}$		0	25 339.2837	-0.05	25 339.290(2) ^b
		1	25 222.2487	0.02	
		2	25 104.7648	-0.18	
$^{91}\text{Zr}^{16}\text{O}$		0	24 986.8280	0.01	
	1	0	25 278.9800	0.08 ^c	
		0	25 290.6416	-0.17 ^c	
$^{92}\text{Zr}^{16}\text{O}$		0	25 318.1075	0.13 ^c	25 256.093(4)
		1	25 256.0960	0.07	
		2	25 139.6384	0.18	
$^{94}\text{Zr}^{16}\text{O}$		0	25 022.7348	-0.05	25 176.414(4)
		1	25 060.5094	-0.05	
		2	24 944.1609	-0.12	
$^{96}\text{Zr}^{16}\text{O}$		0	25 100.0336	0.20	
$^{90}\text{Zr}^{18}\text{O}$		0	22 946.9756	0.03	
		1	22 846.1562	0.05	
		2	22 744.9696	0.39	
$^{92}\text{Zr}^{18}\text{O}$		0	22 863.7702	-0.03	
		1	22 763.4997	-0.32	
		0	22 784.0724	-0.11	

^aFrom least squares fit of data (excluding $^{91}\text{Zr}^{16}\text{O}$ data) to Eq. (2).

^bNumbers in parentheses are the quoted experimental uncertainties.

^cFrom least squares fit of $^{91}\text{Zr}^{16}\text{O}$ data only using SPFIT (Ref. 33).

hypothesis that the splittings would be comparable to those in the spectrum of $^{91}\text{Zr}^{16}\text{O}$, which proved to be the case. Figure 2 illustrates the similar sizes of the nuclear hyperfine splittings for ZrO and ZrS. In the process of measuring the spectrum of $^{91}\text{Zr}^{32}\text{S}$, the $J=1-0$ $v=1$ transition of $^{90}\text{Zr}^{32}\text{S}$ was also found, only 1 MHz from the most intense hyperfine component observed, as shown in Fig. 2. The zirconium sulphide signals were sufficiently strong that transitions in several excited vibrational states of the three most abundant Zr^{32}S isotopomers could be measured, to confirm the identity of this transition. Moreover, the resulting value of α_e for the $X^1\Sigma^+$ state is within 5% of the value of α_e reported for the very low lying $a^3\Delta$ state,¹⁸ which is also the case for the

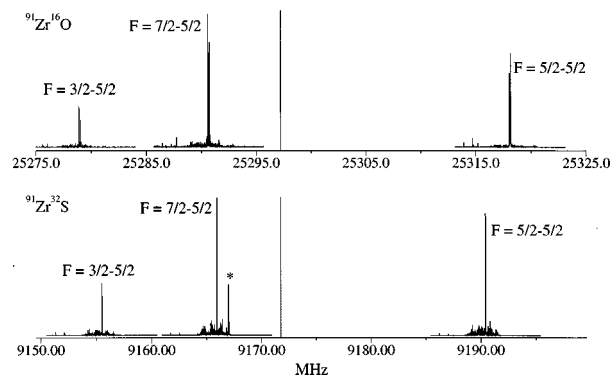


FIG. 2. Two composite spectra showing the nuclear hyperfine structure due to the ^{91}Zr nucleus in the $J=1-0$ transition of $^{91}\text{Zr}^{16}\text{O}$ (upper spectrum) and $^{91}\text{Zr}^{32}\text{S}$ (lower spectrum). The horizontal scales on the two spectra are the same and the hypothetical unsplit frequencies of the $J=1-0$ transitions are shown with dotted lines. The transition marked with an asterisks in the lower spectrum is the $J=1-0$ $v=1$ transition of the main isotopomer $^{90}\text{Zr}^{32}\text{S}$.

TABLE II. Measured frequencies for the $J=1-0$ and $J=2-1$ transitions of ZrS in the $X^1\Sigma^+$ state.

Isotopomer	$F'-F''$	$J'-J''$	v	Frequency (MHz)	obs-calc (kHz) ^a
⁹⁰ Zr ³² S	1-0	0	0	9 198.3007	0.23
	2-1	0	0	18 396.5661	-0.05
	1-0	1	1	9 166.9932	-0.05
	2-1	1	1	18 333.9513	-0.40
	1-0	2	2	9 135.6110	0.00
	2-1	2	2	18 271.1872	-0.01
⁹¹ Zr ³² S	2-1	3	3	18 208.2696	0.04
	1-0	0	0	9 155.5073	0.01 ^b
	1-0	0	0	9 165.9156	-0.01 ^b
	1-0	0	0	9 190.4134	0.00 ^b
	2-1	0	0	18 338.9723	-0.08 ^b
	2-1	0	0	18 340.9603	0.08 ^b
⁹² Zr ³² S	1-0	0	0	9 145.8320	0.12
	2-1	0	0	18 291.6295	0.15
	1-0	1	1	9 114.7928	0.19
	2-1	1	1	18 229.5510	0.18
	1-0	2	2	9 083.6788	-0.39
	2-1	2	2	18 167.3246	0.62
⁹⁴ Zr ³² S	1-0	0	0	9 095.5750	-0.10
	2-1	0	0	18 191.1161	-0.07
	1-0	1	1	9 064.7917	-0.07
	2-1	1	1	18 129.5497	0.18
⁹⁶ Zr ³² S	1-0	2	2	9 033.9345	-0.61
	2-1	2	2	18 067.8360	-0.19
	1-0	0	0	9 047.3995	0.33
	2-1	0	0	18 094.7644	-0.28
⁹⁰ Zr ³⁴ S	1-0	0	0	8 800.0135	0.17
	2-1	0	0	17 599.9947	-0.11

^aFrom least squares fit of data (excluding ⁹¹Zr³²S data) to Eq. (2).

^bFrom least squares fit of ⁹¹Zr³²S data only using SPFIT (Ref. 33).

values of B_0 and ω_e for the two states. The measured transition frequencies for ZrS are given in Table II.

C. ZrS ($a^3\Delta$ state)

The electronic energy of the $a^3\Delta$ state has been predicted by an *ab initio* study¹⁰ to be only $500 \pm 200 \text{ cm}^{-1}$ above that of the $X^1\Sigma^+$ ground state; there is no experimental value for this at present. However, accurate molecular constants for this excited state (for the main isotopomer only) are available from the rotational analyses of the triplet systems of zirconium sulphide.^{18,19} Therefore, since rotational transitions in excited vibrational states up to $\sim 1500 \text{ cm}^{-1}$ above $v=0$ were observed easily, a search was also made for rotational transitions in the $a^3\Delta$ electronic state of ZrS.

The $a^3\Delta$ state is well described by Hund's case (a) coupling and is a regular $^3\Delta$ state.¹⁸ The spin-orbit components are therefore $^3\Delta_1$, $^3\Delta_2$, and $^3\Delta_3$ in order of increasing energy. In each of these spin-orbit components $J \geq \Omega$ and hence the lowest frequency pure rotational transition is $J = (\Omega + 1) - \Omega$. Since B_0 for the $a^3\Delta$ state is approximately $4\,500 \text{ MHz}$, only the $J=2-1$ transition in the $^3\Delta_1$ spin-orbit component at $\sim 18 \text{ GHz}$ is in the frequency range of our spectrometer. Using the effective molecular constants determined for the $^3\Delta_1$ spin-orbit component in Ref. 18 a prediction was made for the $J=2-1$ $v=0$ transition of ⁹⁰Zr³²S. Since no lambda-type doubling had been observed in the

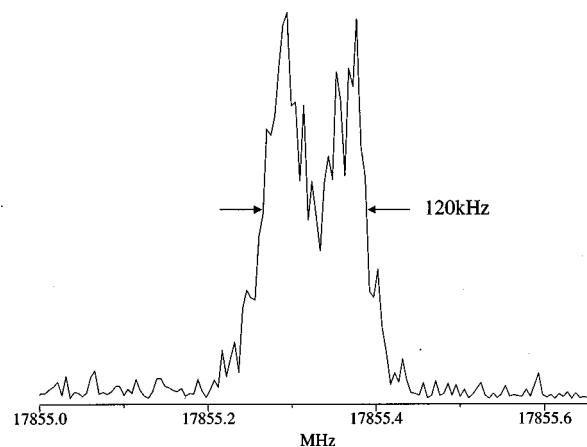


FIG. 3. Power spectrum of the $J=2-1$ $v=0$ transition in the $^3\Delta_1$ spin-orbit component of the $a^3\Delta$ electronic state of ⁹⁰Zr³²S measured in 5000 averaging cycles. The excitation frequency was $17\,855.3340 \text{ MHz}$. 4 K data points were recorded and the power spectrum is shown as a 4 K transformation.

electronic spectrum it was initially assumed to be negligible. Now, the magnetic moment of a molecule, μ , is given by

$$\mu = (\Lambda + g\Sigma)\mu_B, \quad (1)$$

where μ_B = the Bohr Magneton and $g \sim 2$. Therefore, although both Λ and Σ are nonzero in the $^3\Delta_1$ component, since $\Lambda=2$ and $\Sigma=-1$, μ is almost zero. Any Zeeman splitting of the rotational transitions caused by the Earth's magnetic field²⁶ was thus expected to be very small.

A transition was found within 500 kHz of the predicted frequency; it is shown in Fig. 3. The linewidth ($\sim 50 \text{ kHz}$ FWHM) is consistent with a very small, though nonzero, magnetic moment and the intensity is comparable to that of the excited vibrational states, which is consistent with a transition in a low lying electronic state. The assignment of this line was unambiguously confirmed by the observation of the $J=2-1$ transition in the $v=1$ level for the main isotopomer and the $J=2-1$ $v=0$ transition in the ⁹²Zr³²S and ⁹⁴Zr³²S isotopomers. The frequencies of the transitions in the minor isotopomers were predicted by mass scaling the effective molecular constants for ⁹⁰Zr³²S. Again, each of these transitions was found within 500 kHz of the prediction and each line had the characteristic broadened line shape shown in Fig. 3. The line positions of all observed transitions are given in Table III.

TABLE III. Measured frequencies for the $J=2-1$ transition in the $^3\Delta_1$ component of the $a^3\Delta$ state of ZrS.

Isotopomer	v	Frequency
⁹⁰ Zr ³² S	0	17 855.326 9(50) ^a
	1	17 795.697(15)
⁹² Zr ³² S	0	17 753.564(15)
⁹⁴ Zr ³² S	0	17 656.070(15)

^aThe uncertainties have been estimated based on the line shape and relative intensities of the transitions.

TABLE IV. Molecular parameters in megahertz for isotopomers of ZrO in the $X^1\Sigma^+$ state.

parameter ^a	Y_{01}	$10^3 Y_{02}$	Y_{11}	$10^3 Y_{21}$	$10^3 Y_{31}$	δ_{01}^O	δ_{01}^{Zr}	r_e (Å) ^b
	B_e	$-10^3 D_e$	$-\alpha_e$	$10^3 \gamma_e$	$10^3 \epsilon_e$			
⁹⁰ Zr ¹⁶ O ^c	12 698.836 387(350) ^d 12 699.4 ^f	-9.563 ^e -9.56 ^f	-58.295 47(78) -58.58 ^f	-110.4(5) -99 ^f	-0.39(8)	2.696 1(11)	0.378(3)	1.711 952 42(73)
⁹¹ Zr ¹⁶ O ^g	12 677.721 745	-9.531	-58.150 11	-110.0	-0.39			1.711 952 13
⁹² Zr ¹⁶ O	12 657.098 557	-9.500	-58.008 25	-109.7	-0.39			1.711 951 86
⁹⁴ Zr ¹⁶ O	12 617.120 477	-9.440	-57.733 58	-109.0	-0.38			1.711 951 33
⁹⁶ Zr ¹⁶ O	12 578.797 937	-9.383	-57.470 69	-108.3	-0.38			1.711 950 82
⁹⁰ Zr ¹⁸ O	11 498.639 979	-7.840	-50.227 69	-90.5	-0.30			1.711 932 18
⁹² Zr ¹⁸ O	11 456.900 385	-7.784	-49.954 41	-89.9	-0.30			1.711 931 63
⁹⁴ Zr ¹⁸ O	11 416.920 615	-7.729	-49.693 11	-89.2	-0.30			1.711 931 10

Correlation coefficients from least squares fit (isotopomer 1 is ⁹⁰Zr¹⁶O)

Y_{01}	1							
Y_{11}	-0.917	1						rms of residuals=0.15 kHz
Y_{21}	0.869	-0.986	1					no. of data points=17
Y_{31}	-0.832	0.958	-0.991	1				no. of isotopomers=7
δ_{01}^O	0.245	-0.032	0.020	-0.034	1			
δ_{01}^{Zr}	0.419	-0.164	0.143	-0.151	0.312	1		

^aSpectroscopic parameter to which the Y_{k1} is approximately equal, where $E_{v,J}=J(J+1)[B_e - D_e J(J+1) - \alpha_e(v+1/2) + \gamma_e(v+1/2)^2 + \epsilon_e(v+1/2)^3]$; see Ref. 26.

^bCalculated from Y_{01} using $Y_{01}=h/8\pi^2\mu r_e^2$ where μ is the atomic reduced mass.

^cParameters for this isotopomer are the results of the least squares fit of all the isotopic data (excluding ⁹¹Zr¹⁶O data) to Eq. (2). The parameters for all other isotopomers presented in this table are calculated from these using Eq. (5).

^dNumbers in parentheses are 95% confidence limits in units of the last significant figure except those for the bond length r_e , which are one standard deviation in units of the last significant figure (also see text).

^eConstrained to this value (D_0 from Ref. 30) in the fit. The uncertainty quoted is 0.081×10^{-3} MHz; if Y_{02} is constrained to values at the limits of this uncertainty in the fit then Y_{01} varies by less than half the 95% confidence limit given above and the other parameters are unchanged.

^fSpectroscopic parameters from Philips and Davis (Ref. 7). No uncertainties in the parameters are quoted in this reference.

^gData for this isotopomer were not included in the fit and the predicted parameters for this species ignore nuclear spin effects.

IV. ANALYSIS

A. Vibrational data

The analyses of the $X^1\Sigma^+$ state data for the spin-free ($I=0$) isotopomers of ZrO and ZrS were essentially parallel. Initially, the data for each isotopomer were fit separately to spectroscopic constants (B_e , D_e , α_e , etc). Equilibrium bond lengths were then calculated for each isotopomer using the normal relation $B_e = h/8\pi^2\mu r_e^2$. Significantly, the results from this showed that the bond length for the ⁹⁰Zr¹⁸O isotopomer differed from the value obtained from the ⁹⁰Zr¹⁶O isotopomer by 30 times the calculated uncertainty (for example, see Table IV). Such an observation is an indication of breakdown of the Born–Oppenheimer approximation; this effect has been treated by Watson.²⁷ The fact that such a discrepancy in the equilibrium bond lengths of different isotopomers was apparent in the analysis of very accurate yet low J and low v data pointed to the possibility of fitting the FTMW data to a Dunham-like expression.

For this, the program DSParFit, which was kindly provided by Dr. Robert J. Le Roy, was used. This program takes a new approach:²⁸ instead of fitting to a “standard” Dunham-type expansion involving U_{kl} ’s and Δ_{kl} ’s,²⁹ the data are fit to a rearranged form of this expression, from which Y_{kl} and δ_{kl} parameters for the main isotopomer are determined. The explicit expression used for a diatomic AB in a $X^1\Sigma^+$ state is

$$E_{\alpha}(v, J) = \sum_{(kl) \neq (00)} \left(\frac{\mu_1}{\mu_{\alpha}} \right)^{l+k/2} Y_{kl}^1 (v+1/2)^k [J(J+1)]^l + \sum_{(kl) \geq (00)} \left(\frac{\mu_1}{\mu_{\alpha}} \right)^{l+k/2} \left[\left(\frac{M_{\alpha}^{\alpha} - M_A^1}{M_A^{\alpha}} \right) \delta_{kl}^A + \left(\frac{M_B^{\alpha} - M_B^1}{M_B^{\alpha}} \right) \delta_{kl}^B \right] (v+1/2)^k [J(J+1)]^l, \quad (2)$$

where the sub/superscript 1 refers to the main isotopomer, the sub/superscript α refers to any given isotopomer, μ is the reduced mass of the atoms, and M is the atomic mass. Now, experimentally the largest data set is usually obtained for the most abundant (main) isotopomer. One advantage of the above treatment is that the parameters for this isotopomer, rather than a set of U_{kl} ’s, now become the reference point for further corrections. In other words, fitting the data in this way directly produces a set of molecular constants that are relevant to a real system, rather than to the hypothetical potential minimum in the Born–Oppenheimer approximation. The mass-independent parameters describing the latter situation are, of course, directly calculable from the constants obtained using Eq. (2). Furthermore, the atomic mass-dependent Born–Oppenheimer breakdown terms now appear as additive and not multiplicative corrections, and Eq. (2) is therefore linear in the parameters to be determined. The δ_{kl} ’s have the same units as the Y_{kl} ’s and obey the relationship

TABLE V. Molecular parameters in megahertz for isotopomers of ZrS in the $X^1\Sigma^+$ state.

Parameter ^a	Y_{01}	$10^3 Y_{02}$	Y_{11}	$10^3 Y_{21}$	$10^3 Y_{31}$	δ_{01}^S	δ_{01}^{Zr}	$r_e(\text{\AA})^b$
	B_e	$-10^3 D_e$	$-\alpha_e$	$10^3 \gamma_e$	$10^3 \epsilon_e$			
⁹⁰ Zr ³² S ^c	4 606.966 120(320) ^d 4 607.26(16) ^e	-1.45(2) -1.463 0(54) ^e	-15.616 85(67) -15.705 5(50) ^e	-18.17(40)	-0.13(7)	0.516(3)	0.150(2)	2.156 676 49(92)
⁹¹ Zr ³² S ^f	4 593.660 694	-1.44	-15.549 23	-18.07	-0.13			2.156 676 10
⁹² Zr ³² S	4 580.664 958	-1.43	-15.483 29	-17.96	-0.13			2.156 675 73
⁹⁴ Zr ³² S	4 555.472 701	-1.42	-15.355 72	-17.77	-0.13			2.156 675 00
⁹⁶ Zr ³² S	4 531.323 683	-1.40	-15.233 76	-17.58	-0.12			2.156 674 29
⁹⁰ Zr ³⁴ S	4 407.319 808	-1.33	-14.612 63	-16.63	-0.12			2.156 669 40

correlation coefficients from least squares fit (isotopomer 1 is ⁹⁰Zr³²S)

Y_{01}	1							
Y_{11}	-0.855	1						
Y_{21}	0.810	-0.987	1					
Y_{31}	-0.771	0.959	-0.991	1				
Y_{02}	-0.375	-0.032	0.042	-0.054	1			
δ_{01}^S	0.368	-0.251	0.172	-0.155	-0.029	1		
δ_{01}^{Zr}	0.370	-0.176	0.167	-0.178	-0.014	0.399	1	

rms of residuals=0.26 kHz
no. of data points=23
no. of isotopomers=5

^aSpectroscopic parameter to which the Y_{kl} is approximately equal, where $E_{v,J} = J(J+1)[B_e - D_e J(J+1) - \alpha_e(v+1/2) + \gamma_e(v+1/2)^2 + \epsilon_e(v+1/2)^3]$; see Ref. 26.

^bCalculated from Y_{01} using $Y_{01} = h/8\pi^2 \mu r_e^2$ where μ is the atomic reduced mass.

^cParameters for this isotopomer are the results of the least squares fit of all the isotopic data (excluding ⁹¹Zr³²S data) to Eq. (2). The parameters for all other isotopomers presented in this table are calculated from these using Eq. (5).

^dNumbers in parentheses are 95% confidence limits in units of the last significant figure except those for the bond length r_e , which are one standard deviation in units of the last significant figure (also see text).

^eSpectroscopic parameters from Jonsson *et al.* (Ref. 20)

^fData for this isotopomer were not included in the fit and the predicted parameters for this species ignore nuclear spin effects.

$$Y_{kl}^1 = \mu_1^{-(l+k/2)} U_{kl} - \delta_{kl}^A - \delta_{kl}^B, \quad (3)$$

hence in general giving a more obvious picture of the magnitude of the mass-dependent corrections to the Y_{kl}^1 's. It should be noted that δ_{kl} parameters have an implicit dependence on the choice of isotopomer 1. This is best illustrated for the special case of $k=0, l=1$ by the relation of the δ_{01}^1 's to the isotopically independent Watson-type Δ_{01}^1 's

$$\delta_{01}^A = -\frac{m_e U_{01} \Delta_{01}^A}{\mu_1 M_A^1}, \quad (4)$$

where m_e is the mass of the electron, and the analogous equation for atom B . Further advantages are discussed by Le Roy.²⁸

Initially, the FTMW data from this work were least squares fit to Eq. (2) with all the δ_{kl} terms constrained to zero. Since only the $J=1-0$ transition was measured for the ZrO isotopomer, Y_{02}^1 was constrained to the value of the centrifugal distortion parameter $-D_0$ for the main isotopomer given by Balfour and Tatum,³⁰ which is essentially the same as $-D_e$ given by Philips and Davis⁷ (see Table IV). For both molecules, the residuals in the resulting fits had unacceptably large root-mean-square (rms) values: 258 kHz for ZrO and 23 kHz for ZrS. This demonstrates that, particularly in the case of ZrO, simple mass scaling of the Y_{kl} parameters is completely inadequate to model the data. Only the inclusion of both the δ_{01}^S and δ_{01}^{Zr} terms reduced the rms of the residuals below the estimated measurement uncertainty (± 1 kHz); no other δ_{kl} or Y_{kl} terms could be determined for either molecule. The parameters and correlation coefficients resulting from these fits of the ZrO and ZrS data

are given in Tables IV and V, respectively; the residuals are given in Tables I and II, respectively. It can be seen that the δ_{01} parameters obtained from these fits are all well determined and are not highly correlated with any other parameters. This indicates that using FTMW data alone, a breakdown in the Born–Oppenheimer approximation for these two molecules can be observed. In particular, for ZrO, even measurement of only the $J=1-0$ transition has demonstrated that the effect is real and that it can be quantified.

It should be noted that the above analysis fitted the data to well within the experimental uncertainty without the inclusion of the nuclear field effects described by Schlembach and Tiemann.³¹ These had been found to be significant for metal atoms low in the periodic table, notably Tl and Pb,³¹ in several diatomics. Since DSParFit is not yet programmed to include these effects, the program used in the initial fitting was modified and extended to check that the nuclear field effects could be ignored. Only the effect of the Zr nucleus was included. It was found that the inclusion of the field effect did not improve the rms of the residuals, and furthermore produced a fitting constant that was indeterminate and was essentially perfectly correlated with δ_{Zr}^{01} . A fit was also tried in which the field effect was included but δ_{Zr}^{01} was ignored, following the procedure of Ref. 31. In this case the rms of the residuals was ten times worse, and greater than the experimental uncertainty, and systematic isotopically dependent residuals were found. We thus conclude that the nuclear field effects can be ignored with the present data, though a larger data set might possibly reveal them. The following discussions are based on this assumption.

TABLE VI. Molecular constants in megahertz for $^{91}\text{Zr}^{16}\text{O}$ and $^{91}\text{Zr}^{32}\text{S}$.

Molecule	B_0	$10^3 D_0$	$eQq_0(^{91}\text{Zr})$	$C_I(^{91}\text{Zr})$
$^{91}\text{Zr}^{16}\text{O}$	12 648.619 15 ^a	9.531 ^a	130.549 9(46) ^b	-0.014 15(23)
$^{91}\text{Zr}^{32}\text{S}$	4 585.881 68(41)	1.455(66)	116.460 9(47)	-0.011 03(24)

^aConstrained to these values; see text.

^bNumbers in parentheses are one standard deviation in units of the last significant figure.

For both species, Y_{kl} 's were determined for the main isotopomers directly in the least squares fits, the results of which are given in Tables IV and V. Y_{kl} 's for the minor isotopomers have been calculated using the results of the fit and

$$Y_{kl}^\alpha = \left\{ Y_{kl}^1 + \left(\frac{M_A^\alpha - M_A^1}{M_A^\alpha} \right) \delta_{kl}^A + \left(\frac{M_B^\alpha - M_B^1}{M_B^\alpha} \right) \delta_{kl}^B \right\} \left(\frac{\mu_1}{\mu_\alpha} \right)^{l+k/2}, \quad (5)$$

and are also given in Tables IV and V for the reader's convenience. In addition, r_e values have been calculated from the Y_{01} parameters to demonstrate the variation in "equilibrium bond lengths" between isotopomers of the same molecular species. As a note, the uncertainties in the r_e bond lengths quoted here are dominated by the uncertainties in the fundamental constants,³² not by those in the atomic masses or Y_{01} 's.

It should be borne in mind, however, that because of the limited data set, the parameters obtained in the present work are likely to model only the bottom of the potential well effectively and that as a result their predictive powers for higher J and v transitions are probably limited. Unfortunately, no vibration-rotation spectra have been recorded for either species to date to test this hypothesis. However, combining the data obtained in the current study with existing information on the $X^1\Sigma^+$ state from electronic spectroscopy and fitting them together to directly determine a potential would be desirable.

B. Hyperfine structure

The spectroscopic constants for the $^{91}\text{Zr}^{16}\text{O}$ and $^{91}\text{Zr}^{32}\text{S}$ isotopomers were determined using Pickett's exact fitting program SPFIT (Ref. 33) and are given in Table VI. This program employs a Hamiltonian of the form

$$\mathbf{H} = \mathbf{H}_{\text{rotation}} + \mathbf{H}_{\text{cent. distortion}} + \mathbf{H}_{\text{nuc. quadrupole}} + \mathbf{H}_{\text{nuc. spin-rotation}} \\ = B_0 \mathbf{J}^2 - D_0 \mathbf{J}^4 + \mathbf{V}^{(2)} \cdot \mathbf{Q}^{(2)} + C_I \mathbf{I} \cdot \mathbf{J}. \quad (6)$$

For $^{91}\text{Zr}^{32}\text{S}$ a sufficient number of transitions were observed so that all four constants given in Table IV could be determined directly in a least squares fit. By comparing Eq. (2) with the above Hamiltonian it can be seen that numerically in this case $B_0 = Y_{01} - \frac{1}{2}Y_{11} - \frac{1}{4}Y_{21} - \frac{1}{8}Y_{31}$ and $D_0 = -Y_{02}$. The B_0 and D_0 parameters determined for $^{91}\text{Zr}^{32}\text{S}$ in this way are therefore in excellent agreement with the results of the multi-isotopomer fit (Table V) which predict $B_0 = 4585.881\,544$ MHz and $D_0 = 1.442 \times 10^{-3}$ MHz.

In the case of $^{91}\text{Zr}^{16}\text{O}$, however, only three hyperfine components were measured. In order to determine values for

TABLE VII. Watson-type Δ_{01} terms for several diatomics.

Molecule(AB)	Δ_{01}^A	Δ_{01}^B	Ref.
ZrO	-4.872(39) ^a	-6.188 8(25)	this work
ZrS	-5.325(82)	-6.523(39)	this work
CO	-2.054 5(12)	-2.098 2(13)	34
GeSe	-1.505(87) ^b	-1.86(14) ^b	35
GaH	-2.62(35)	-4.218 1(13)	36
ClH	-0.26(20)	0.126 2(8)	37

^aThe numbers in parentheses are one standard deviation in units of the last significant figure.

^bThese numbers are actually Δ_B terms determined from a fit to Dunham potential parameters, but only differ from Δ_{01} terms in that they do not contain a contribution from the Dunham correction, which is expected to be small.

both eQq_0 and C_I from the data the parameters in Table IV were used to calculate values for the constants B_0 and D_0 for the $^{91}\text{Zr}^{16}\text{O}$ isotopomer and these were constrained in the fit. This is equivalent to calculating and constraining the hypothetical unsplit transition frequency and modeling the hyperfine interaction only. In the resulting fit the residuals had a rms of 0.13 kHz which is very satisfactory and illustrates the quality of the results in Table IV.

V. DISCUSSION

A. Born-Oppenheimer breakdown (BOB) correction terms

To our knowledge, the present work is the first time that (BOB) correction terms have been obtained for a transition metal-containing diatomic; the results are particularly interesting. In order to facilitate comparisons with other species, the Watson-type Δ_{01} terms have been calculated for ZrO and ZrS from the constants in Tables IV and V and are given in Table VII. This also provides the advantage of a comparison of isotopically independent parameters for which there are expressions already in the literature for the various contributions. The BOB terms determined in this work for both of the atoms in the each of the zirconium species studied are large when compared to those of other molecules for which this type of analysis has been performed; several such results are also given in Table VII. Many previous studies have been concerned with either very light molecules or hydrides [since the correction terms are proportional to $1/M$ as can be seen from Eq. (2)]; however the present work shows that the effects of the breakdown of the Born-Oppenheimer approximation are also evident for the transition metal oxide and sulphide studied here. Three previous studies of relatively heavy metal oxides [BaO and SrO,³⁸ SnO,³⁹ and GeO (Ref. 40)], which all combined infrared and microwave data, were unable to determine rotational BOB parameters for either atom. However, they have been determined for PbS and several other group 13 and 14 diatomics; see Ref. 41.

Following Tiemann *et al.*⁴¹ the Δ_{01} correction terms may be written

$$\Delta_{01} = \Delta_{01}^{\text{ad}} + \Delta_{01}^{\text{nonad}} + \Delta_{01}^{\text{Dunham}}, \quad (7)$$

which for atom A, for example, becomes

$$\Delta_{01}^A = (\Delta_{01}^A)^{\text{ad}} + \frac{(\mu g_J)_B}{m_p} + \frac{\mu \Delta Y_{01}^{(D)}}{m_e B_e}, \quad (8)$$

where $(\Delta_{01}^A)^{\text{ad}}$ is the adiabatic correction to the Born–Oppenheimer approximation, $(\mu g_J)_B$ is the isotopically independent value of μg_J referred to nucleus B as origin, m_p is the mass of the proton and $\Delta Y_{01}^{(D)}$ is the Dunham correction to Y_{01} . The last term in Eq. (8) can be calculated from available spectroscopic constants.^{27,26} It is found to be of the order of 10^{-8} MHz for each term in both ZrO and ZrS, and therefore negligible at the accuracy considered here. Hence the experimentally determined values of the Δ_{01} 's in this work can be viewed as simply the sum of the adiabatic and nonadiabatic contributions. Unfortunately, the molecular rotational g_J factor has not been measured for either species and so the relative magnitude of these two contributions for each atom cannot be quantified yet. However, considering the electronic structures of these molecules (which are typical of transition metal species) it does seem likely that the dominant contributions to these BOB terms for both the Zr and the O and S atoms will be nonadiabatic in origin. In addition to the second-order interaction of the $X^1\Sigma^+$ state with excited $^1\Pi$ states treated by Watson,²⁹ it is also possible that other second order (e.g., spin orbit) and a number of higher-order terms would be significant for these transition metal compounds given the large number of low-lying electronic states that are present. For example, in ZrS there are seven known electronic states (two single, five triplet) within $\sim 15\,000\text{ cm}^{-1}$ of the ground state. In particular the very low-lying ($\sim 500\text{ cm}^{-1}$) $a^3\Delta$ state could interact with the ground state via the $B^1\Pi$ state at around $10\,000\text{ cm}^{-1}$. Since the magnitude of the correction due to this interaction is proportional to the inverse of the energy differences between the states this might be expected to be significant. It will be interesting to see if similar results are obtained for other transition metal diatomic species.

B. Bond lengths

The determination of BOB terms in this work leads to the need for a clear definition of what is meant by a bond length. The r_e values given in Tables IV and V were calculated directly from the Y_{01} 's (which are strictly only approximately equal to B_e) using the atomic reduced mass and will be referred to as the ‘‘atomic equilibrium bond lengths.’’ When the Dunham correction can be neglected (as in this case) then $Y_{01} = B_e$ and so this bond length can also be viewed as $r_e^{\text{(ad+nonad)}}$. It differs between isotopomers because both the adiabatic and nonadiabatic contributions to the Born–Oppenheimer bond length are isotopically dependent. The previous literature values of the bond lengths defined in this way for the main isotopomers are presented for comparison in Table VIII.

The isotopically invariant Born–Oppenheimer bond length, r_e^{BO} , can be calculated for each molecule using

$$U_{01} = \frac{h}{8\pi^2 (r_e^{\text{BO}})^2}, \quad (9)$$

TABLE VIII. Calculation of bond lengths in angstroms for ZrO and ZrS.

	⁹⁰ Zr ¹⁶ O	⁹⁰ Zr ³² S
r_e	1.711 952 42(73) ^a	2.156 676 49(92)
r_e^{BO}	1.711 745 27(74)	2.156 520 76(92)
r_e^{lit}	1.711 91 ^b	2.156 61(4) ^c

^aThe numbers in parentheses are one standard deviation in units of the last significant figure.

^bCalculated from B_e given by Philips and Davis (Ref. 7) using the atomic reduced mass.

^cJonsson *et al.* (Ref. 20).

given by Bunker,⁴² since U_{01} is obtained from the constants in Tables IV and V using Eq. (3). This number represents what the bond length for a molecule would be if the first-order Bohr–Sommerfeld quantization condition is assumed to be exact and mass dependent corrections to the potential energy function are ignored. It also given in Table VIII. It is interesting to note that the values of r_e^{BO} for ZrO and ZrS differ from those for r_e for the main isotopomer significantly, by $\sim 2 \times 10^{-4}\text{ \AA}$ in both cases. This is comparable to the uncertainties in the literature values of the r_e bond lengths determined by electronic spectroscopy for these isotopomers. This difference is, of course, a mass-dependent effect; the corresponding differences for some other species are found to be $\sim 4 \times 10^{-5}\text{ \AA}$ for HCl,²⁷ $\sim 1 \times 10^{-4}\text{ \AA}$ for CO,²⁷ and $\sim 2 \times 10^{-3}\text{ \AA}$ for GaH.³⁶

As mentioned in Sec. V A, the nonadiabatic effects cannot be calculated because of the lack of the molecular g_J factor [see Eqs. (10) and (21) in Ref. 27). However, having calculated r_e^{BO} , a very crude approximation for g_J may be obtained with the assumption that nonadiabatic effects completely dominate and therefore $r_e^{\text{ad}} \approx r_e^{\text{BO}}$. The result is $g_J = -0.44$ for ZrO and -0.27 for ZrS.

C. Quadrupole coupling constants

It is clear from Table VI that the ⁹¹Zr quadrupole coupling constants for ZrS and ZrO have the same signs and are very similar in magnitude. This is also true for the spin rotation parameters for the two molecules. In order to understand the various contributions to the $eQq_0(^{91}\text{Zr})$ parameter for each species, a useful starting point is a qualitative molecular orbital diagram. Figure 4 shows such a diagram for ZrO. In this picture¹⁰ the bonding is described in terms of fully occupied 11σ and 5π molecular orbitals largely localized on the oxygen which arise primarily from the oxygen $2p$ and the zirconium $4d$ atomic orbitals. The remaining two valence electrons occupy the 12σ orbital, a zirconium-centered $5s5p$ hybrid pointing away from the oxygen, thus reducing electron–electron repulsion. It is possible to derive an expression for $eQq_0(^{91}\text{Zr})$ in terms of the contributions from unbalanced electrons (both p and d) using the Townes–Dailey model⁴³ and an extension of this model given by Brown.⁴⁴ The resulting expression in this case is

$$eQq_0(^{91}\text{Zr}) = eQq_{510}n_{5p_z} + eQq_{420} \left[n_{4d_{z^2}} + \frac{(n_{4d_{xz}} + n_{4d_{yz}})}{2} \right], \quad (10)$$

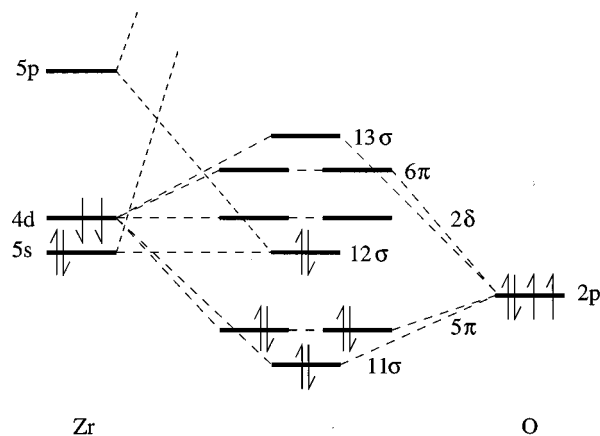


FIG. 4. Qualitative molecular orbital diagram for ZrO.

where eQq_{510} and eQq_{420} are the zirconium atomic quadrupole coupling constants for a single electron in a $5p$ or $4d$ orbital, respectively, and n_i is the number of electrons in the zirconium i atomic orbital (the z axis being along the internuclear bond). Neither eQq_{510} nor eQq_{420} is available in the literature; however, there is an experimental value of $\langle r^{-3} \rangle_{4d} = 2.30a_0^{-3}$ for the $4d^25s^2$ configuration.⁴⁵ Using this value and the expression

$$eQq_{nl0}(\text{MHz}) = -2.353 \frac{2l(l+1)}{(2l+3)(2l-1)} \times Q(fm^2) \langle (a_0/r)^3 \rangle, \quad (11)$$

derived from Gordy and Cook²⁶ a value of $eQq_{420} = +63.7$ MHz is obtained. The number of electrons in the zirconium $5p_z$ orbital can be estimated if the degree of hybridization of the 12σ orbital is known. While there is no direct measure of this for the $X^1\Sigma^+$ state, the magnetic hyperfine parameter b_F for the $a^3\Delta$ state for ZrO has been used to deduce the percentages of $5s$ (39%) and hence $5p$ (61%) character of the corresponding orbital in that electronic state.⁸ If it is assumed that the degree of hybridization is the same in both these electronic states and also that two electrons occupy this orbital, this then gives a value for n_{5p_z} of 1.21. This leaves as unknowns in Eq. (10) eQq_{510} and the populations of the three $4d$ orbitals involved in bonding. Here, two possible solutions of Eq. (10) are presented.

In the first, the $4d\sigma$ and $4d\pi$ populations (0.75 and 0.92, respectively) calculated in the *ab initio* study by Langhoff and Bauschlicher¹⁰ are substituted into Eq. (10) and $eQq_{510} = +44.2$ MHz is obtained. This leads to $\langle r^{-3} \rangle_{5p} = 1.14a_0^{-3}$, which is considerably smaller than the value for $\langle r^{-3} \rangle_{4d}$. Such a result is qualitatively consistent with recent results for Ti where $\langle r^{-3} \rangle_{3d} = 1.4a_0^{-3}$ from atomic measurements⁴⁶ and $\langle r^{-3} \rangle_{4p} = 0.4a_0^{-3}$ from Fletcher *et al.*⁴⁷ A similar trend is also observed for Sc.⁴⁸ Although this result is not conclusive, it is at least consistent with the current understanding of the bonding in transition metal diatomics.

A second approach involves making the assumption that, based on the above discussion, an upper limit for the value of $\langle r^{-3} \rangle_{5p}$ for Zr is obtained by setting it equal to the experimental value for $\langle r^{-3} \rangle_{4d}$. This would then give an upper

limit for the first term on the right hand side of Eq. (10) and hence a lower limit for the second term and consequently the minimum populations for the $4d$ orbitals. By assuming that the populations of all three orbitals are equal we have $n_{4d_z} = n_{4d_{xz}} = n_{4d_{yz}} = 0.18$. By referring back to the molecular orbital diagram in Fig. 4 it can then be calculated that the maximum charge transfer from zirconium to oxygen on formation of ZrO would then be approximately one and a half electrons. In other words, the upper limit on the ionicity of the molecule is in the region $Zr^{+1.5}O^{-1.5}$. It should be noted that the *ab initio* study¹⁰ determined the net charge on Zr to be +0.36; however this calculation underestimated both the dipole moment of ZrO [1.560 D compared to the experimental value of 2.551 (11) D (Ref. 9)] and the degree of $5s5p$ hybridization.

The size of $eQq_0(^{91}\text{Zr})$ is similar for ZrS and ZrO although *ab initio* calculations predict ZrS to be appreciably less ionic than ZrO.¹⁰ The magnetic hyperfine parameters for the $a^3\Delta$ state of ZrS have not been measured and so an identical treatment for ZrS is not possible. However, the results can be rationalized in terms of the bonding because in each case there are two effects which contribute to the magnitude of $eQq_0(^{91}\text{Zr})$. Sulphur is less electronegative than oxygen suggesting that there would be less charge transfer on formation of an ionic bond. Thus the negative sulphide ion would generate a smaller electrostatic field than the oxide ion and so the Zr electron distribution would be less polarized by it. Hence it seems likely that there would be less $5p$ character in the sp hybrid on Zr in ZrS than in ZrO. This would tend to decrease the experimentally determined value of $eQq_0(^{91}\text{Zr})$. On the other hand, there would probably be greater overlap of atomic orbitals between Zr and S than between Zr and O because of the greater spatial extent of sulphur orbitals. This would lead to a greater covalent component in the bonding and increased zirconium $4d$ occupancy, thus causing an increase in the observed value of $eQq_0(^{91}\text{Zr})$. The former effect presumably dominates in this case resulting in a slightly smaller value for $eQq_0(^{91}\text{Zr})$ in ZrS than ZrO.

D. $a^3\Delta$ state of ZrS

It is interesting to note that both ZrO and ZrS have a $^1\Sigma^+$ ground state while both TiO and TiS have a $^3\Delta$ ground state. The $^3\Delta$ state in all these species arises from the promotion of one electron from the metal centered sp hybrid to the vacant metal $d\delta$ orbital. The reduction in electron-electron repulsion offsets the energy required for electronic promotion. In ZrS the electronic energy of the $a^3\Delta$ state is of the order of the vibrational interval and so it is not surprising that transitions within this state could be observed in this experiment. The relative strengths of the transitions observed in the two electronic states in this work remove any doubt that the ground state of ZrS is indeed the $^1\Sigma^+$ state.

The line shape of the transitions observed in the $a^3\Delta$ state suggests that there is some unresolved Zeeman splitting of the $J=2-1$ line. Unfortunately our Helmholtz coils are not sufficiently well aligned to collapse down the structure of such a small splitting. In addition to this, unresolved lambda-

type doubling may also contribute to the broadening of the lines. A search of 30 MHz either side of the $J=2-1$ $v=0$ transition of the main isotopomer revealed no lambda-type doubling partner to that transition. If the doubling were larger than this, then it would certainly have been resolved at higher J in the electronic spectrum, which was not the case. Hence it is concluded that for all the transitions observed in this work, the lambda-type doubling is within our experimental linewidth. In the limit of pure case (a) coupling and the absence of any Zeeman splitting, this places an upper limit on the lambda-type doubling parameter $\tilde{\delta}_\Delta$ (Ref. 49) of approximately 6 kHz.

VI. CONCLUSION

ZrO and ZrS have been generated using a laser ablation/supersonic expansion technique and their rotational spectra have been recorded using FTMW spectroscopy. Transitions in six isotopomers of zirconium monosulphide and eight isotopomers of zirconium monoxide have been observed. The data obtained in this work were fit to a Dunham-like expression and from the results Born–Oppenheimer breakdown correction terms and equilibrium bond distances have been determined. Not only has this work produced the determination of BOB terms for a transition metal-containing diatomic, it has done so using only FTMW data. Hyperfine parameters for the $^{91}\text{Zr}^{32}\text{S}$ and $^{91}\text{Zr}^{16}\text{O}$ species have also been determined and used to investigate the participation of d electrons in the bonding of these molecules. A pure rotational transition in the $a^3\Delta$ state of ZrS has also been observed providing some information on the lambda-type doubling in this state.

ACKNOWLEDGMENTS

This work has been supported by the Natural Sciences and Engineering Research Council of Canada (NSERC). The authors thank Dr. Robert J. Le Roy for the program DSParFit and for valuable discussions and extensive comments on the manuscript. They thank the authors of Ref. 20 for communicating their results to them prior to publication. They also acknowledge Drs. Anthony Merer, Kaley Walker, Richard Suenram, and Dale Brugh for helpful discussions.

¹A. J. Merer, *Annu. Rev. Phys. Chem.* **40**, 407 (1989).

²H. Spinrad and R. F. Wing, *Annu. Rev. Astron. Astrophys.* **7**, 249 (1969).

³P. C. Keenan, *Astrophys. J.* **107**, 420 (1948).

⁴H. L. Nordh, B. Lindgren, and R. F. Wing, *Astron. Astrophys.* **56**, 1 (1977).

⁵D. L. Lambert and R. E. S. Clegg, *Mon. Not. R. Astron. Soc.* **191**, 367 (1980).

⁶P. W. Merrill, *Astrophys. J.* **56**, 457 (1922).

⁷J. G. Phillips and S. P. Davis, *Astrophys. J.* **229**, 867 (1979).

⁸B. Simard, S. A. Mitchell, L. M. Hendel, and P. A. Hackett, *Faraday Discuss. Chem. Soc.* **86**, 163 (1988).

⁹R. D. Suenram, F. J. Lovas, G. T. Fraser, and K. Matsumura, *J. Chem. Phys.* **92**, 4724 (1990).

¹⁰S. R. Langhoff and C. W. Bauschlicher, Jr., *J. Chem. Phys.* **89**, 2160 (1988).

¹¹S. R. Langhoff and C. W. Bauschlicher, Jr., *Astrophys. J.* **349**, 369 (1990).

¹²P. D. Hammer and S. P. Davis, *J. Mol. Spectrosc.* **78**, 337 (1979).

¹³J. E. Littleton and S. P. Davis, *Astrophys. J.* **296**, 152 (1985).

¹⁴P. C. Keenan, *Astrophys. J.* **55**, 74 (1950).

¹⁵B. Simard, S. A. Mitchell, M. R. Humphries, and P. A. Hackett, *J. Mol. Spectrosc.* **129**, 186 (1988).

¹⁶B. Simard, S. A. Mitchell, and P. A. Hackett, *J. Chem. Phys.* **89**, 1899 (1988).

¹⁷J. Jonsson, B. Lindgren, and A. G. Taklif, *Astron. Astrophys.* **246**, L67 (1991).

¹⁸J. Jonsson, *J. Mol. Spectrosc.* **169**, 18 (1995).

¹⁹J. Jonsson and B. Lindgren, *J. Mol. Spectrosc.* **169**, 30 (1995).

²⁰J. Jonsson, S. Wallin, and B. Lindgren, *J. Mol. Spectrosc.* **192**, 198 (1998).

²¹L. Karlsson and C. Lundevall, *J. Phys. B* **31**, 491 (1998).

²²T. J. Balle and W. H. Flygare, *Rev. Sci. Instrum.* **52**, 33 (1981).

²³Y. Xu, W. Jäger, and M. C. L. Gerry, *J. Mol. Spectrosc.* **151**, 206 (1992).

²⁴K. A. Walker and M. C. L. Gerry, *J. Mol. Spectrosc.* **182**, 178 (1997).

²⁵L. Karlsson, B. Lindgren, C. Lundevall, and U. Sassenberg, *J. Mol. Spectrosc.* **181**, 274 (1997).

²⁶W. Gordy and R. L. Cook, *Microwave Molecular Spectra*, 3rd ed. (Wiley, New York, 1984).

²⁷J. K. G. Watson, *J. Mol. Spectrosc.* **45**, 99 (1973).

²⁸R. J. Le Roy, *J. Mol. Spectrosc.* (submitted).

²⁹J. K. G. Watson, *J. Mol. Spectrosc.* **80**, 411 (1980).

³⁰W. J. Balfour and J. B. Tatum, *J. Mol. Spectrosc.* **48**, 313 (1973).

³¹J. Schlembach and E. Tiemann, *Chem. Phys.* **68**, 21 (1982).

³²I. Mills, T. Cvitaš, K. Homann, N. Kallay, and K. Kuchitsu, *Quantities, Units and Symbols in Physical Chemistry*, 3rd ed. (Blackwell Scientific, Oxford, 1993).

³³H. M. Pickett, *J. Mol. Spectrosc.* **148**, 371 (1991).

³⁴N. Authier, N. Bagtland, and A. Le Floch, *J. Mol. Spectrosc.* **160**, 590 (1993).

³⁵T. Honno and H. Uehara, *Chem. Phys. Lett.* **247**, 529 (1995).

³⁶J. M. Campbell, M. Dulick, D. Klapstein, J. B. White, and P. F. Bernath, *J. Chem. Phys.* **99**, 8379 (1993).

³⁷G. Guelachvili, P. Niay, and P. Bernage, *J. Mol. Spectrosc.* **85**, 271 (1981).

³⁸C. E. Blom, H. G. Hedderich, F. J. Lovas, R. D. Suenram, and A. G. Maki, *J. Mol. Spectrosc.* **152**, 109 (1992).

³⁹A. G. Maki and F. J. Lovas, *J. Mol. Spectrosc.* **98**, 146 (1983).

⁴⁰E. G. Lee, J. Y. Seto, T. Hirao, P. F. Bernath, and R. J. Le Roy, University of Waterloo Chemical Physics Research Report CP-636 (1998).

⁴¹E. Tiemann, H. Arnst, W. U. Stieda, T. Törring, and J. Hoefl, *Chem. Phys.* **67**, 133 (1982).

⁴²P. R. Bunker, *J. Mol. Spectrosc.* **68**, 367 (1977).

⁴³C. H. Townes and B. P. Dailey, *J. Chem. Phys.* **17**, 782 (1949).

⁴⁴T. L. Brown, *Acc. Chem. Res.* **7**, 408 (1974).

⁴⁵S. Büttgenbach, R. Dicke, H. Gebauer, R. Kuhn, and F. Träber, *Z. Phys. A* **286**, 125 (1978).

⁴⁶R. Aydin, E. Stachowska, U. Johann, and J. Dembezczyński, *Z. Phys. D* **15**, 281 (1990).

⁴⁷D. A. Fletcher, C. T. Scurlock, K. Y. Jung, and T. C. Steimle, *J. Chem. Phys.* **99**, 4288 (1993).

⁴⁸T. C. Steimle, A. J. Marr, and D. M. Goodridge, *J. Chem. Phys.* **107**, 10406 (1997).

⁴⁹J. M. Brown, A. S.-C. Cheung, and A. J. Merer, *J. Mol. Spectrosc.* **124**, 464 (1987).